AMERICAN SOCIETY FOR MICROBIOLOGY | mBio®

RESEARCH ARTICLE
Host-Microbe Biology

The Gene Expression Profile of Uropathogenic *Escherichia coli* in Women with Uncomplicated Urinary Tract Infections Is Recapitulated in the Mouse Model

Arwen E. Frick-Cheng,[a] Anna Sintsova,[a,b] Sara N. Smith,[a] Michael Krauthammer,[b] Kathryn A. Eaton,[a] Harry L. T. Mobley[a]

[a]Department of Microbiology and Immunology, University of Michigan, Ann Arbor, Michigan, USA
[b]Department of Quantitative Biomedicine, University of Zurich, Zurich, Switzerland

Arwen E. Frick-Cheng and Anna Sintsova contributed equally to this work. Author order was determined alphabetically.

ABSTRACT Uropathogenic *Escherichia coli* (UPEC) is the primary causative agent of uncomplicated urinary tract infections (UTIs). UPEC fitness and virulence determinants have been evaluated in a variety of laboratory settings, including a well-established mouse model of UTI. However, the extent to which bacterial physiologies differ between experimental models and human infections remains largely understudied. To address this important issue, we compared the transcriptomes of three different UPEC isolates in human infection and under a variety of laboratory conditions, including LB culture, filter-sterilized urine culture, and the UTI mouse model. We observed high correlation in gene expression between the mouse model and human infection in all three strains examined (Pearson correlation coefficients of 0.86 to 0.87). Only 175 of 3,266 (5.4%) genes shared by all three strains had significantly different expression levels, with the majority of them (145 genes) downregulated in patients. Importantly, gene expression levels of both canonical virulence factors and metabolic machinery were highly similar between the mouse model and human infection, while the *in vitro* conditions displayed more substantial differences. Interestingly, comparison of gene expression between the mouse model and human infection hinted at differences in bladder oxygenation as well as nutrient composition. In summary, our work strongly validates the continued use of this mouse model for the study of the pathogenesis of human UTI.

IMPORTANCE Different experimental models have been used to study UPEC pathogenesis, including *in vitro* cultures in different media, tissue culture, and mouse models of infection. The last is especially important since it allows evaluation of mechanisms of pathogenesis and potential therapeutic strategies against UPEC. Bacterial physiology is greatly shaped by environment, and it is therefore critical to understand how closely bacterial physiology in any experimental model relates to human infection. In this study, we found strong correlation in bacterial gene expression between the mouse model and human UTI using identical strains, suggesting that the mouse model accurately mimics human infection, definitively supporting its continued use in UTI research.

KEYWORDS UPEC, transcriptome, human infection, mouse model of UTIs, UPEC

Urinary tract infections (UTIs) are among the most common bacterial infections in otherwise healthy individuals. Over 50% of women experience at least one UTI in their lifetime, and half of these women experience a recurrent infection within a year (1, 2). These infections affect 150 million people per year and result in annual medical costs of $3.5 billion in the United States alone (3). Uropathogenic *Escherichia coli* (UPEC) is responsible for 80% of uncomplicated UTIs (1) and deploys diverse strategies to

Citation Frick-Cheng AE, Sintsova A, Smith SN, Krauthammer M, Eaton KA, Mobley HLT. 2020. The gene expression profile of uropathogenic *Escherichia coli* in women with uncomplicated urinary tract infections is recapitulated in the mouse model. mBio 11:e01412-20. https://doi.org/10.1128/mBio.01412-20.

Editor Vanessa Sperandio, University of Texas Southwestern Medical Center Dallas

Address correspondence to Harry L. T. Mobley, hmobley@med.umich.edu.

Received 1 June 2020
Accepted 7 July 2020
Published 11 August 2020

survive and replicate in the human host. These comprise an array of virulence factors, including, but not limited to, iron acquisition systems (siderophores and heme receptors), fimbriae and other adhesins, flagella, and toxins (4–7). The importance of these systems to bacterial fitness has been studied in detail using multiple models, including cultures in laboratory media, human urine cultures, tissue culture, and a mouse model first established over 30 years ago (8). However, animal models can fail to recapitulate important aspects of the human response to disease (9). Whether the mouse model accurately reflects the native environment found during human infection has not been adequately addressed. Therefore, it is vitally important to determine if the mouse model of ascending UTI recapitulates human UTI since defining mechanisms of pathogenesis and the development of UTI therapies rely on this assumption (10).

Previous studies compared the mouse model to human UTIs using microarrays to assess differences in bacterial gene expression (11, 12). Initially, urine from mice infected with UPEC type strain CFT073 was collected over a period of 10 days, pooled, and analyzed using a microarray based on the CFT073 genome (11). In a follow-up study, urine was collected from eight women with complicated UTIs and bacterial gene expression in the human host was analyzed, again using microarrays based on the CFT073 genome (12). Relative expression levels of 46 fitness genes were compared between the mouse model and human UTI. This comparison demonstrated a Pearson's correlation coefficient of 0.59 and was strongest for iron acquisition systems and weakest for adhesin and motility systems (12). While encouraging, this study did not provide conclusive evidence that the mouse model closely replicated human UTI. A key weakness of the previous comparison was that genetic differences between currently circulating isolates and strain CFT073 used for the mouse infections would obscure strain-specific responses, either due to differences in mouse versus human UTI or because the CFT073-specific microarrays would not detect expression of genes that are not encoded by that strain.

We have recently used RNA sequencing (RNA-seq) to quantify the UPEC transcriptome during acute infection in 14 female patients (13). Importantly, RNA-seq is a more comprehensive platform to analyze the transcriptome of clinical UPEC strains since, unlike microarrays, it is not limited by strain-specific probes. Here, we report the transcriptome during murine UTI for 3 of the 14 clinical strains using RNA-seq and direct comparison of the gene expression patterns for these identical strains between human UTI and the mouse model. We observed a high correlation between human infection and mouse infection (Pearson correlation coefficient ranging from 0.86 to 0.87), with only 175 of 3,266 shared genes being differentially expressed. Gene expression of classical virulence factors as well as metabolic genes in the mouse model closely resembled those observed during human UTI. Our study is the first of its kind to directly compare the bacterial transcriptomes between human and mouse UTIs using identical strains. We conclude that the mouse model accurately reflects bacterial gene expression observed during human infection.

RESULTS

Study design. We previously sequenced the transcriptomes of 14 UPEC strains isolated directly from the urine of patients with uncomplicated UTIs (hUTIs) and immediately stabilized with RNAprotect (13). Three out of 14 strains (HM43, HM56, and HM86) were chosen to conduct transcriptomic studies in the prevailing mouse model of UTI (mUTI) (8). We selected strains whose hUTI transcriptomes had the highest proportion of bacterial reads to eukaryotic reads (see Table S1 in the supplemental material) and that possessed a prototypical UPEC virulence factor profile. All three strains belong to the B2 phylogroup (13), which includes the majority of UPEC strains and encode a range of siderophores, heme receptors, and multiple fimbrial types (Fig. 1).

To compare UPEC gene expression levels during mUTI and hUTI, 40 mice were transurethrally inoculated with each UPEC strain and mouse urine was collected directly into RNAprotect, 48 h postinoculation (hpi), for RNA isolation and sequencing. Animals

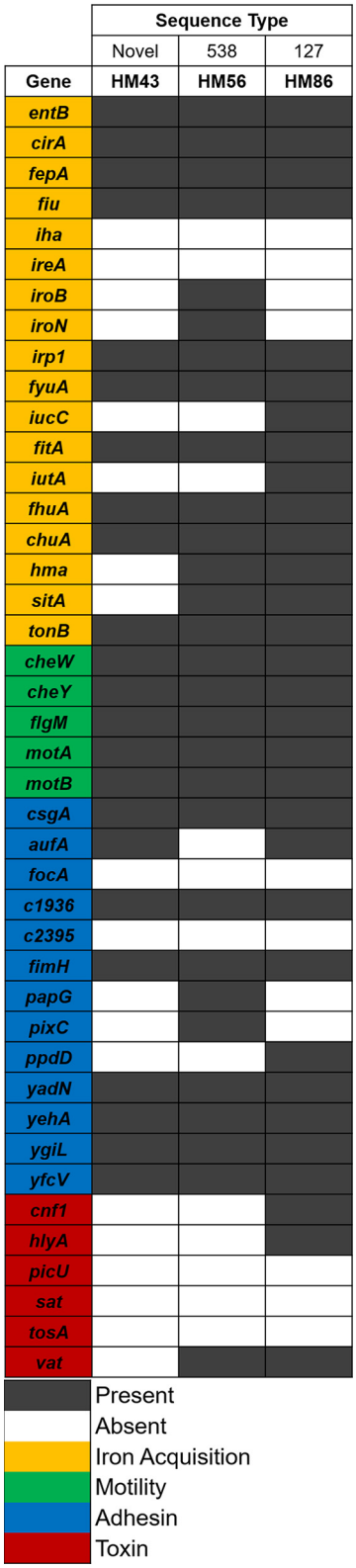

FIG 1 Virulence factors present in selected clinical UPEC strains. Presence or absence of these 42 genes was determined via BLAST (≥80% coverage and ≥90% identity). White indicates absence of the gene, while black indicates presence. Color coding on gene names identifies the function of each virulence factor. Goldenrod is iron acquisition, green is motility, blue is adhesins, and red is toxins. Sequence types were determined computationally and reported by Sintsova et al. (13).

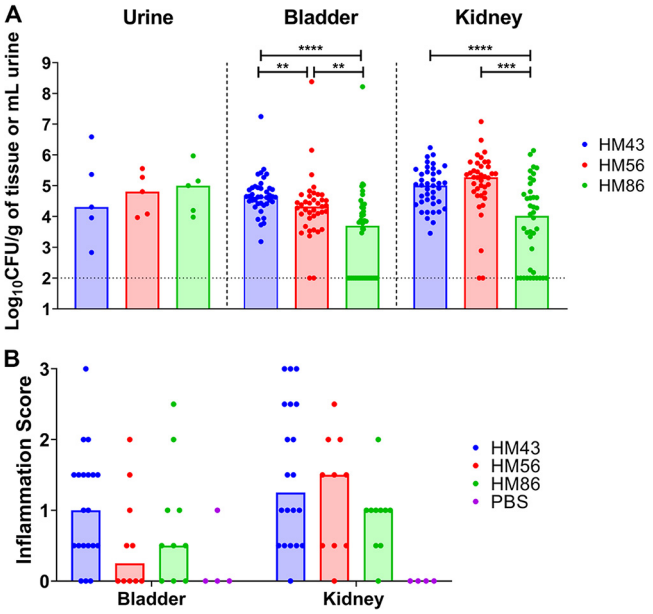

FIG 2 Murine colonization and inflammatory response of selected clinical UPEC strains. CBA/J mice were transurethrally inoculated with 10^8 CFU of the indicated strain (HM43, HM56, or HM86). (A) Bacterial burden was enumerated from urine, bladder, and kidneys 48 h postinfection. Symbols represent individual animals, and bars represent the medians. The dotted line indicates limit of detection. A two-tailed Mann-Whitney test was performed to test significance. **, $P < 0.01$; ***, $P < 0.005$; ****, $P < 0.0001$. (B) Inflammation was assessed using histopathological analysis of stained thin sections of each specified organ. Inflammation was scored on a scale of 0 to 3, with 0 being no inflammation and 3 being severe inflammation. Mice were mock infected with PBS to serve as a negative control. Symbols represent individual animals, and bars represent the medians.

were then sacrificed and the bacterial burdens of their urine, bladders, and kidneys were quantified. All three strains successfully colonized the animals, with bacterial burdens ranging between 5.0×10^3 and 4.4×10^4 CFU/g in the bladder and 1×10^4 and 1.2×10^6 CFU/g in the kidneys (Fig. 2A), levels of colonization that are consistent with an active UTI. We also assessed levels of inflammation (on a scale from 0 to 3) in the bladders and kidneys of these infected mice, comparing them to those of mice that were mock infected with phosphate-buffered saline (PBS) (Fig. 2B and Fig. S1). After 48 h, infection with all of the three UPEC strains resulted in mild levels of inflammation in the bladder (median inflammation scores of 1.0, 0.25, and 0.5 for HM43, HM56, and HM86, respectively) and slightly higher levels in the kidneys (median inflammation scores of 1.25, 1.5, and 1.0 for HM43, HM56, and HM86, respectively). These similar scores indicated that the general host responses were comparable across these three different strains.

In addition to isolating RNA from mouse urine during mUTI, we also isolated and sequenced RNA from HM43, HM56, and HM86 cultured to mid-logarithmic phase in both filter-sterilized human urine and lysogeny broth (LB). All samples processed in this study underwent identical treatments to deplete eukaryotic mRNA, prepare libraries, and conduct sequencing (see Materials and Methods).

The bacterial transcriptome is highly correlated between human and mouse infections. First, we assessed how UPEC gene expression during hUTI compared to that under *in vitro* conditions and during mUTI. For each strain, we compared $\log_2$ transcripts per million (TPMs) of every gene between LB and hUTI, human urine culture and hUTI, and, finally, mUTI and hUTI. Gene expression during hUTI and mUTI was most highly correlated with the Pearson correlation coefficient (r), ranging from 0.86 to 0.87 (Fig. 3). In contrast, the *in vitro* human urine culture compared to hUTI exhibited lower correlation values, 0.73 to 0.80 (Fig. 3), consistent with our previous report (13). Interestingly, gene expression correlation between LB and hUTI was higher than the

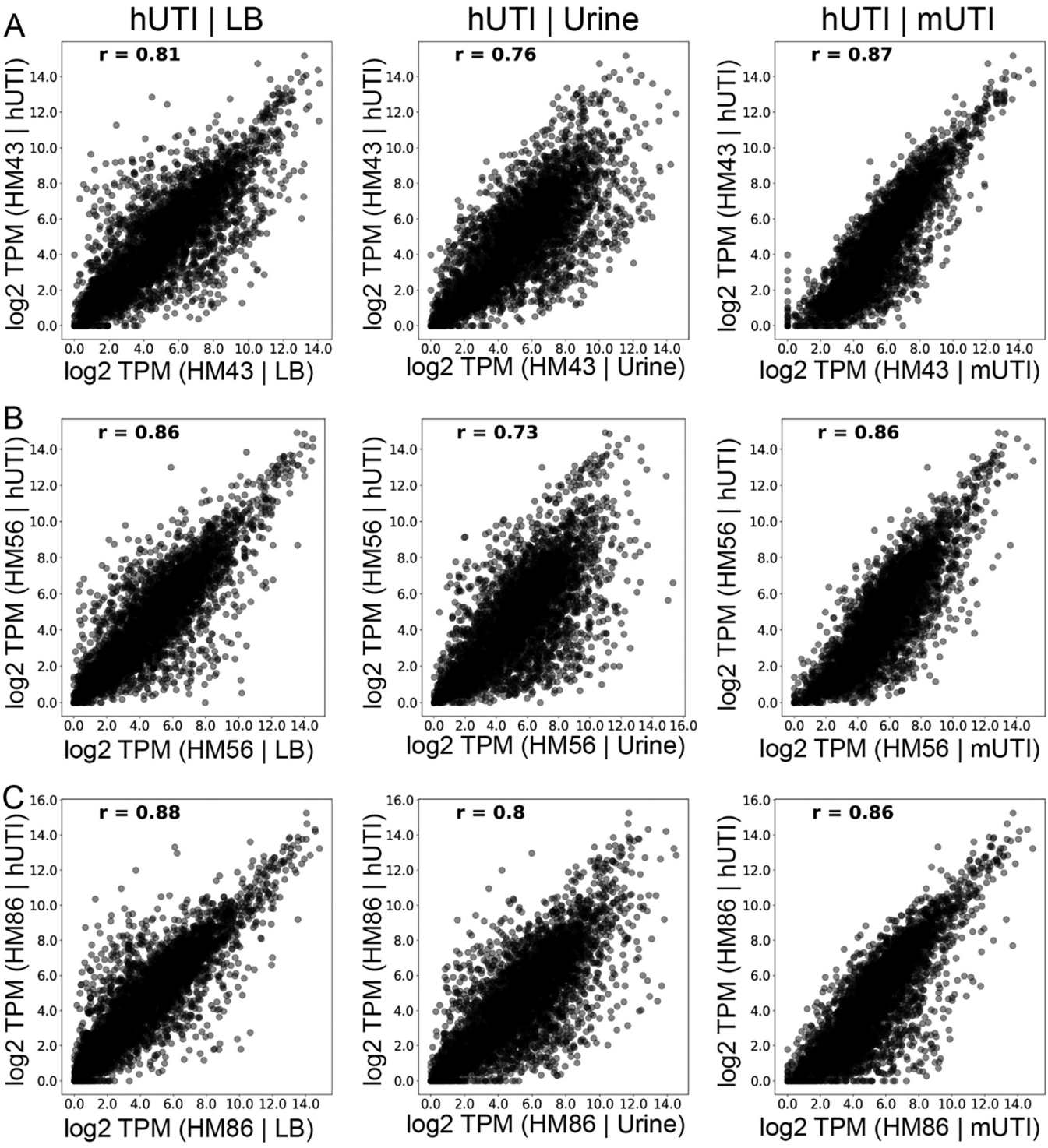

FIG 3 UPEC gene expression during mouse and human infections is highly correlated. Normalized levels of gene expression (log_2 TPM) for three UPEC strains—HM43 (A), HM56 (B), and HM86 (C)—were compared between LB culture and human infection (hUTI | LB), urine culture and human infection (hUTI | urine), and mouse infection and human infection (hUTI | mUTI). Pearson correlation coefficient (*r*) is shown in the top left corner of each plot.

correlation between urine and hUTI (*r* between 0.80 and 0.88) (Fig. 3). Our data demonstrate that murine infection is the most reliable and consistent model to recapitulate the conditions that are observed during human infection.

Contribution of growth rate to gene expression patterns. We have recently shown that diverse UPEC strains show a conserved gene expression pattern in human

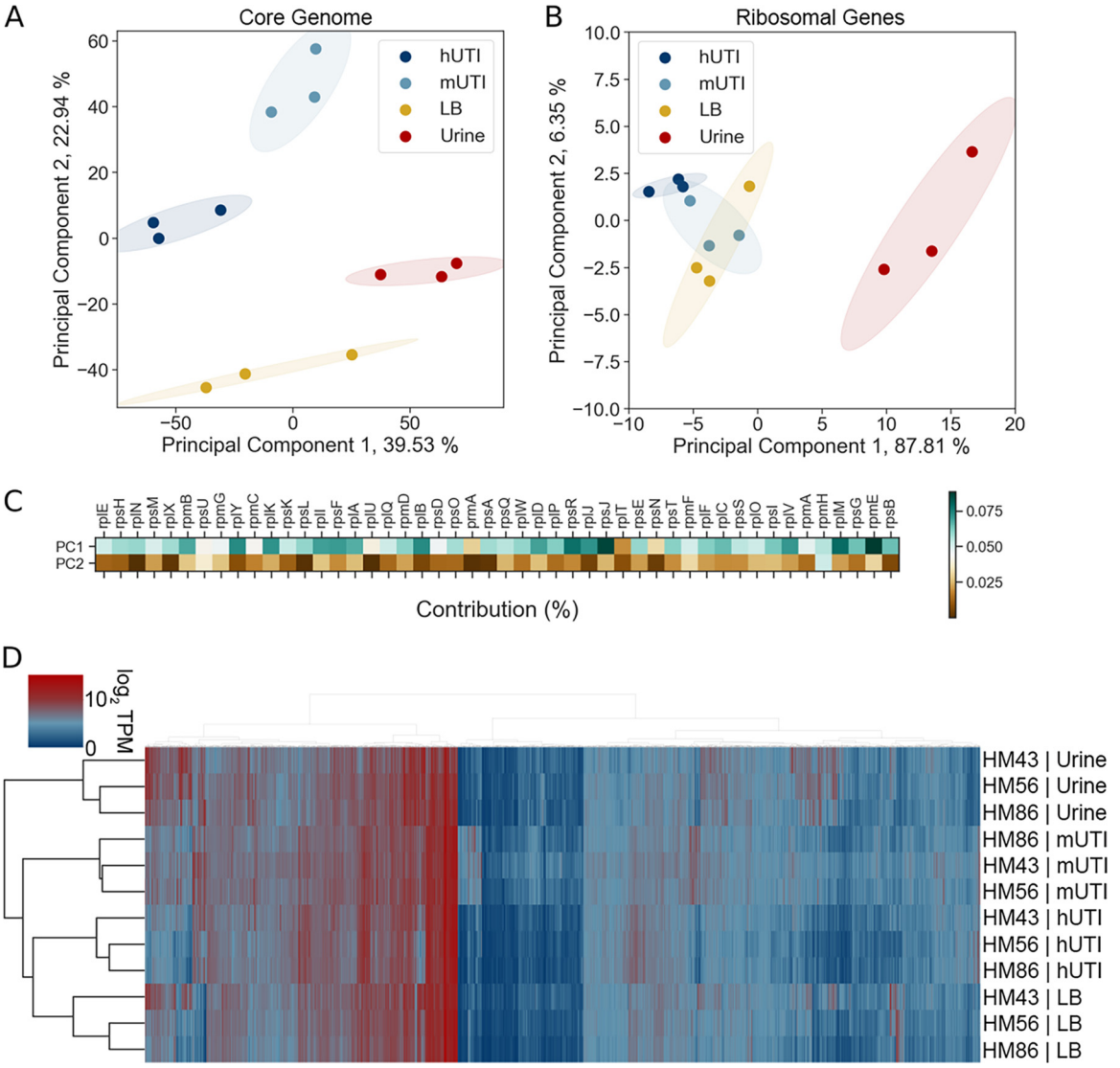

FIG 4 Host-associated gene expression is distinct from that of *in vitro* culture. (A) Principal-component analysis of normalized gene expression of 3 clinical UPEC strains during human infection (hUTI), during mouse infection (mUTI), during *in vitro* LB culture (LB), and in *in vitro* urine cultures (urine). (B) Principal-component analysis of normalized r-protein expression of 3 clinical UPEC strains during human infection (hUTI), during mouse infection (mUTI), during *in vitro* LB culture (LB), and in *in vitro* urine cultures. (C) Percent contribution from r-proteins to PC1 and PC2 from the PCA shown in panel A. (D) Hierarchical clustering of *in vitro*, murine, and patient samples based on normalized gene expression of genes present in all 3 strains ($n = 3,266$).

patients with uncomplicated UTIs (13). Since we saw such strong correlation between gene expression in patients and in mice for each of the UPEC strains (Fig. 3), we hypothesized that we would also observe a conserved pattern of gene expression between different UPEC strains during mUTI. To address this hypothesis, we performed principal-component analysis (PCA) on gene expression of the 3,266 genes present in all three UPEC strains (Fig. 4A). We observed four distinct clusters that corresponded to the two *in vitro* growth conditions (LB and filter-sterilized human urine cultures) and the two infection hosts (human patients and mice) all displaying condition-specific gene expression programs. Samples from patients and mice clustered closer to each other than to *in vitro* samples, suggesting that there is an infection-specific gene expression pattern conserved between the two hosts.

We further wanted to estimate the contribution of growth rate to similarity of gene expression profiles between mUTI and hUTI since a major hallmark of the conserved transcriptional program of UPEC in humans is rapid growth (13–15). When cultured *in*

vitro, there was no appreciable difference in the growth rates of the UPEC strains cultured in human urine (Fig. S2A and B). There appeared to be an extremely subtle difference in growth rate in LB between HM43 and HM86 (Fig. S2C and D), which is interesting given that these two strains had the largest difference in correlation between hUTI and LB (*r* values of 0.81 and 0.88, respectively). However, while HM86 had the highest correlation, it grew more slowly than HM43, indicating that it is potentially more than just growth rate that drives this similarity.

We also performed PCA using only ribosomal protein expression data (Fig. 4B), since expression of ribosomal proteins is directly correlated with bacterial growth rate (16, 17), as another method to dissect the contribution of growth rate. While this analysis showed a clear difference between urine samples and other conditions, it failed to clearly separate LB, mUTI, and hUTI samples (Fig. 4B). This suggests that while growth rate undoubtedly shapes the gene expression pattern in mUTI and hUTI, growth rate alone is insufficient to explain gene expression patterns observed in Fig. 3 and 4A. Additionally, we looked at how much each of the ribosomal genes contributed to the either principal component 1 (PC1) or principal component 1 (PC2) (Fig. 4C). We found that all of the ribosomal genes contributed more to PC1 than to PC2 values. Thus, we hypothesize that PC1 might in fact separate samples based on growth rate, while other unknown factors account for sample separation along PC2.

The conclusions of PCA (clear separation of samples based on condition rather than on strain) were independently confirmed using Ward's hierarchical clustering of $\log_2$ TPM values (Fig. 4D). We also demonstrate that growth in rich medium (LB) more closely mimics hUTI than growth in nutrient-poor human urine, in agreement with the previously demonstrated rapid growth of UPEC in the host (both mouse and human) compared to that in human urine (13–15, 18).

Differentially regulated genes between human and mouse infection suggest nutritional disparities. Despite the high concordance of hUTI and mUTI gene expression data, we wanted to determine whether any genes are differentially regulated between human and mouse infections. To answer this question, we used the R package DEseq2 (19) to find significant differences in gene expression between the two different infections. Strikingly, only 175 genes, representing 5.4% of the 3,266 genes analyzed, were differentially regulated (30 upregulated and 145 downregulated) in human infection compared to the mouse model (Fig. 5A, Tables 1 and 2, and Table S2).

The upregulated gene with the highest $\log_2$ fold change difference (4.3) between humans and mice was *cspA*, which encodes an RNA chaperone initially identified as a cold shock protein (20, 21). However, this protein may have other functions, as it is highly expressed during early exponential phase (22) and during the introduction of fresh nutrient sources (23). In addition, one of the genes responsible for cell division, *ftsB*, and a major regulator of rRNA transcription, *fis*, were upregulated in hUTI compared to mUTI.

The majority of differentially regulated genes were downregulated in patients compared to mice, and several of these genes span operons encompassing specific systems (Table 2 and Table S2). For example, during mUTI, we observed increased expression of the citrate lyase operon *citCDEFGTX*, which is responsible for the conversion of citrate oxaloacetate and acetate and feeds into the production of acetyl coenzyme A (acetyl-CoA) under anaerobic conditions (24), the pathway for allantoin breakdown (*allABDC*), and ethanolamine utilization (*eutABCDEGHJLMNPQST*) (Table 2 and Table S2). In addition, genes encoding transporters for the uptake of L-arabinose (*araADFGH*), L-ascorbate (*ulaABCDEDF*), and allantoin (*ybbW*) were transcribed at higher levels during mUTI (Table 2 and Table S2). Furthermore, several genes related to anaerobic metabolism or fermentation (*hycBDF* and *frdAB*) were more highly expressed in mice (Table 2 and Table S2). All of these results indicate subtle nutrient differences between the mouse and human urinary tracts.

Infection-specific gene expression. Additionally, we were interested in identifying genes that behaved similarly during both human and mouse infections, i.e., genes that

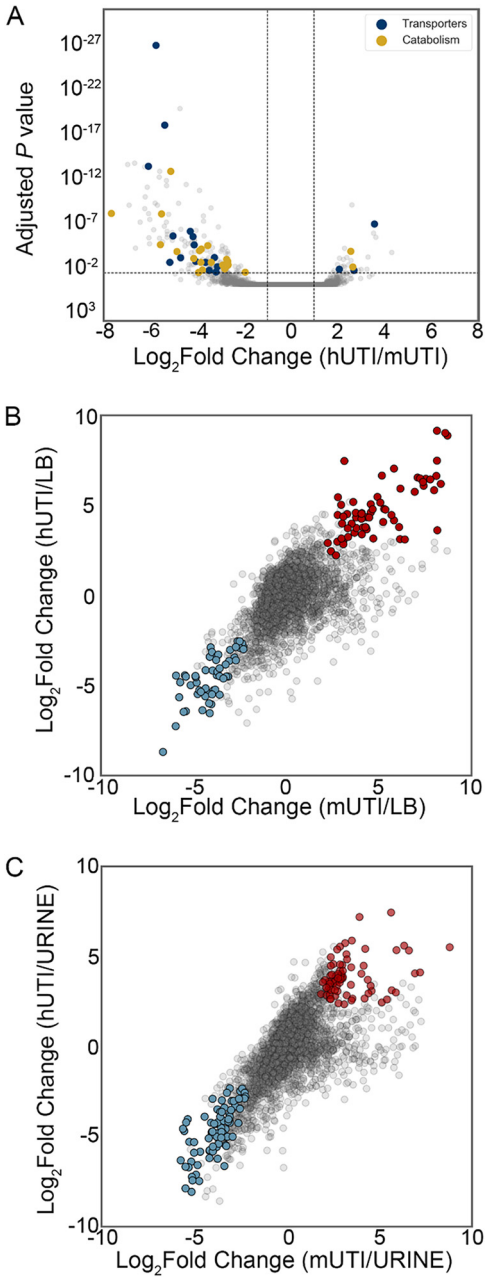

FIG 5 Differential expression analysis reveals infection-specific gene expression responses. (A) The DESeq2 R package was used to compare UPEC gene expression during mUTI to that in patients. Each UPEC strain was considered an independent replicate ($n = 3$). Genes were considered upregulated (downregulated) if the $\log_2$ fold change in expression was higher (lower) than 1 (vertical lines) and the *P* value was <0.05 (horizontal line). Using these cutoffs, we identified 30 upregulated genes and 145 downregulated genes in patients. GO/pathway analysis showed a number of transporters and catabolic enzymes among differentially expressed genes. (B and C) Identification of genes differentially expressed during infection (hUTI or mUTI) compared to LB (B) or urine (C). Genes were considered to be up- or downregulated in both mice and humans if the $\log_2$ fold change was higher or lower than 1 and the *P* value was <0.05 in both cases. Genes that were upregulated during infection compared to LB (B) or urine (C) are shown in red, and genes that were downregulated during infection compared to LB are shown in blue.

were up- or downregulated in both mouse and human UTIs compared to either of the *in vitro* conditions (LB or filter-sterilized human urine). There were 54 downregulated genes in both mouse and human UTIs compared to LB (Fig. 5B and Table S3), and there were 67 upregulated genes during both mUTI and hUTI compared to LB (Fig. 5B and

TABLE 1 Genes differentially upregulated in human patients and mice

Gene	Annotation	Log_2 FC[a]	Locus tag
ahpC	Alkyl hydroperoxide reductase, AhpC component	2.6	b0605
cspA	Cold shock protein CspA	4.3	b3556
dsdX	D-Serine transporter	2.7	b2365
fis	DNA-binding transcriptional dual regulator Fis	2.4	b3261
ftsB	Cell division protein FtsB	2.3	b2748
gntK	D-Gluconate kinase, thermostable	2.7	b3437
gpt	Xanthine-guanine phsophoribosyltransferase	2.4	b0238
gspH	Hypothetical type II secretion protein GspH	3.0	UTI89_C3381
gspL	Hypothetical type II secretion protein GspL	3.3	UTI89_C3377
hpt	Hypoxanthine phosphoribosyltransferase	2.1	b0125
ibaG	Acid stress protein IbaG	2.2	b3190
lysP	Lysine:H(+) symporter	2.1	b2156
opgC	Protein required for succinyl modification of osmoregulated periplasmic glucans	2.6	b1047
ribE	6,7-Dimethyl-8-ribityllumazine synthase	2.1	b0415
rpmE	50S ribosomal subunit protein L31	2.7	b3936
suhB	Inositol phosphate phosphatase	2.6	b2533
yajG	Putative lipoprotein YajG	2.6	b0434
yceA	UPF0176 protein YceA	3.5	b1055
yciB	Inner membrane protein	2.3	b1254
ydiE	PF10636 family protein YdiE	2.1	b1705
yecJ	DUF2766 domain-containing protein YecJ	2.5	b4537
yejL	DUF1414 domain-containing protein YejL	2.2	b2187
yfaZ	Putative porin YfaZ	2.9	b2250
yfhL	Putative 4Fe-4S cluster-containing protein YfhL	2.6	b2562
yghD	Putative type II secretion system M-type protein	3.6	b2968
yghG	Lipoprotein YghG	3.3	b2971
yifK	Putative transporter YifK	3.6	b3795
yqcC	DUF446 domain-containing protein YqcC	2.5	b2792
yqgF	Ribonuclease H-like domain-containing nuclease	2.3	b2949
yqiA	Esterase YqiA	2.3	b3031

[a]FC, fold change.

Table S3). Interestingly, both chemotaxis (*cheABWYZ*) and flagellar machinery (*flgCFGLM* and *fliS*) were downregulated during infection, which may be attributed to the fact that the UPEC strains we analyzed were isolated from the urine of infected individuals; motility genes tend to be upregulated when UPEC enters the ureters to ascend to the kidneys (25). In contrast, *nrdEFHI* genes are upregulated in both mice and humans compared to LB. These genes encode ribonucleotide reductases required for DNA synthesis, and therefore often associated with fast growth, fitting the previously established paradigm of UPEC's high *in vivo* growth rate during human and murine infections (13–15, 18).

There were 82 genes that were downregulated during either mUTI or hUTI compared to urine (Fig. 5C and Table S4). These included branched-chain amino acid biosynthesis (*ilvCDEMN*) and leucine biosynthesis (*leuABCD*) operons, consistent with previous literature indicating that UPEC scavenges amino acids and peptides during infection (13, 26). In contrast, there were 72 genes that were upregulated in humans and mice compared to urine (Fig. 5C and Table S4). As previously reported (13), we observed 16 genes associated with ribosomal subunit production as well as the master regulator *fis*, which activates rRNA transcription, together reinforcing our observation that bacteria grow rapidly in the host (13, 14).

Expression of fitness factors during murine infection is predictive of gene expression during human infection. Finally, we wanted to determine whether previously identified UPEC virulence factors that have been studied using *in vivo* mouse models would show comparable levels of expression during both mouse and human infections. We focused on three major functional groups of fitness factors: iron acquisition systems, adhesins, and metabolism (Table S5). We plotted log_2 TPMs of the genes in each functional group, comparing expression between hUTI and LB, hUTI and urine, and hUTI and mUTI for each of the UPEC strains (Fig. 6 and Fig. S3).

TABLE 2 Top 30 genes differentially downregulated in human patients and mice

Gene	Annotation	Log_2 FC	Locus tag
allB	Allantoinase	−7.0	b0512
allD	Ureidoglycolate dehydrogenase	−6.0	b0517
araA	L-Arabinose isomerase	−5.6	b0062
citC	Citrate lyase synthetase	−6.2	b0618
citD	Citrate lyase acyl carrier protein	−5.6	b0617
citG	Triphosphoribosyl-dephospho-CoA synthase	−5.5	b0613
citX	Apo-citrate lyase phosphoribosyl-dephospho-CoA transferase	−5.9	b0614
eutG	Putative alcohol dehydrogenase in ethanolamine utilization	−5.7	b2453
eutM	Putative structural protein, ethanolamine utilization microcompartment	−6.1	b2457
eutN	Putative carboxysome structural protein	−6.6	b2456
fdrA	Putative acyl-CoA synthetase FdrA	−6.2	b0518
frdA	Fumarate reductase flavoprotein subunit	−5.6	b4154
frdB	Fumarate reductase iron-sulfur protein	−5.3	b4153
frdC	Fumarate reductase membrane protein FrdC	−6.1	b4152
glxR	Tartronate semialdehyde reductase 2	−7.7	b0509
hycA	Regulator of the transcriptional regulator FhlA	−5.3	b2725
hycB	Formate hydrogenlyase subunit HycB	−6.0	b2724
ompW	Outer membrane protein W	−6.4	b1256
ssnA	Putative aminohydrolase	−5.3	b2879
tdcA	DNA-binding transcriptional activator TdcA	−6.2	b3118
tdcB	Catabolic threonine dehydratase	−5.5	b3117
ulaA	L-Ascorbate-specific PTS enzyme IIC component	−6.1	b4193
ulaB	L-Ascorbate-specific PTS enzyme IIB component	−5.8	b4194
ulaC	L-Ascorbate-specific PTS enzyme IIA component	−5.4	b4195
ybbW	Putative allantoin transporter	−6.7	b0511
ygeW	Putative carbamoyltransferase YgeW	−6.9	b2870
ygeY	Putative peptidase YgeY	−6.1	b2872
ygfK	Putative oxidoreductase, Fe-S subunit	−5.8	b2878
yhjX	Putative pyruvate transporter	−5.4	b3547
ylbE	DUF1116 domain-containing protein YlbE	−5.6	b4572

As expected, iron acquisition gene expression was much higher during human infection than during growth in rich LB medium (Fig. 6A). The expression levels were more similar between urine culture (an iron-poor medium) and human infection, but murine infection provided the most analogous profile (Fig. 6A). The only adherence gene cluster that was highly expressed under any of the assayed conditions was the *fim* operon, which encodes type 1 fimbriae. Expression of *fim* genes was higher in patients than under either of the *in vitro* conditions but almost perfectly matched the expression levels observed during mouse infection (Fig. 6B).

Anaerobic metabolic genes showed a major difference between human infection and *in vitro* growth. The converse is also true; aerobic respiration genes, in particular, were expressed at lower levels in humans than under either *in vitro* condition. Importantly, we also observed that the expression levels of aerobic respiration genes aligned concordantly between humans and mice (Fig. 6C), while anaerobic respiration gene expression was elevated in mice compared to that in humans. This observation corroborates results in Fig. 5A, Table 2, and Table S2, where several genes involved in anaerobic metabolism were expressed at higher levels in mice than in hUTI. Overall, we conclude, with only limited exceptions, that the mouse model of UTI not only shows a strong global correlation of gene expression with hUTI but also closely reflects the expression of virulence and fitness genes that are known to contribute to UPEC fitness during human infection.

DISCUSSION

UPEC virulence factors as well as potential therapeutic strategies have been studied in detail using a well-established mouse model of ascending UTI that involves transurethral inoculation of UPEC into the bladder. This mouse model has been extensively used in the field, and the original papers defining this model (8, 27) have been cited nearly 500 times. While this model has been the gold standard in the field to relate scientific discovery to human health, there are some differences between the experi-

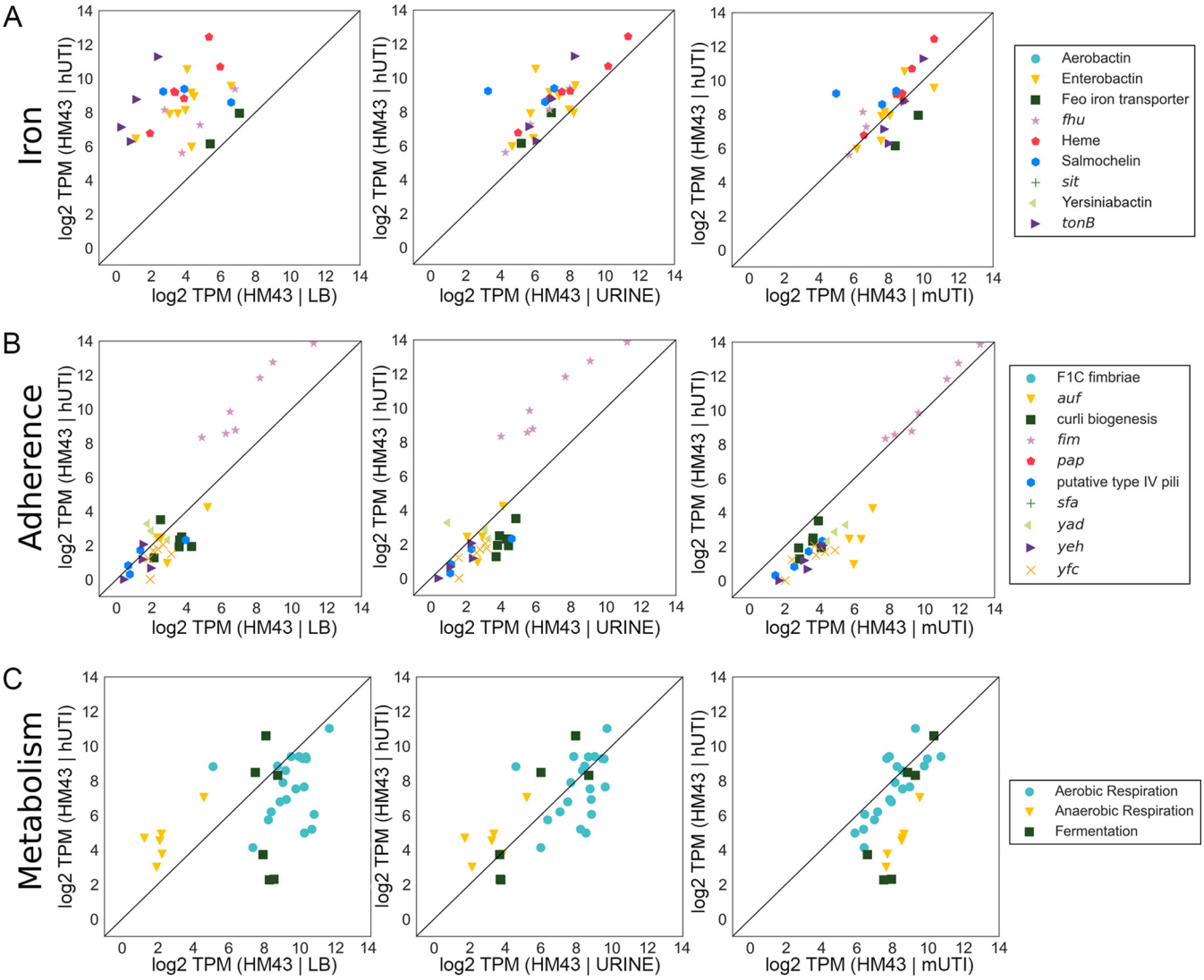

FIG 6 Gene expression of virulence factors as well as metabolic machinery is highly consistent between the mouse model of UTI and human UTI. Normalized levels of gene expression of iron acquisition operons (A), adherence genes (B), and metabolic pathways (C) for HM43 were compared between LB and human infection (LB | hUTI), urine and human infection (urine | hUTI), and mouse UTI and human UTI (mUTI | hUTI).

mental model and what occurs in human infection. In the murine model, $>10^7$ CFU are inoculated directly into the mouse bladder, while in human infection, the number of infecting bacteria is likely to be far lower and bacteria are not directly introduced into the bladder. Rather, it is thought that in humans, the periurethral region is transiently colonized by UPEC and bacteria ascend to the bladder and, in some cases, to the kidneys (28). Furthermore, there are some differences in the immune responses between mice and humans. For example, mice express Toll-like receptor 11 (TLR11), which induces host inflammation in response to UPEC and provides the kidneys with a modest level of protection from bacterial colonization (29). However, humans do not express TLR11 (29), indicating that not all murine responses precisely mimic the human response. Therefore, it is of the utmost importance to validate the murine model of UTI and understand the extent to which it recapitulates human disease. Until now, there has been no direct comparison of global bacterial gene expression between human and mouse studies using the identical strain, and it is essential to understand how the mouse model relates to human disease. This study is the first to define the bacterial transcriptome from infected patients and infected mice using the same UPEC strain, thus presenting a direct comparison between the murine model and human infection.

Our study demonstrates that the UTI mouse model accurately recapitulates the human disease with respect to the bacterial transcriptional response.

We compared three UPEC strains (HM43, HM56, and HM86) that were isolated in 2012 from women with symptoms of cystitis and documented significant bacteriuria (30). We isolated bacterial RNA, stabilized immediately, from their urine to conduct RNA-seq and define the core bacterial transcriptome during acute human infection (13). The same strains were then used for mouse infection, followed by urine collection, bacterial RNA isolation, and sequencing. We consistently observed a high correlation between the bacterial transcriptome during mouse and human infections, with the Pearson correlation coefficient ranging from 0.86 to 0.87. This correlation is not strain specific, as infections with all three stains showed similar results. Levels of expression of virulence and metabolic genes were also found to be very similar between human and mouse infections. While all three strains belonged to the B2 phylogroup, we do not believe this to be a phylogroup-specific effect, as we have previously shown few differences in gene expression between different UPEC phylogroups (13). This provides strong evidence that the mouse model is an accurate representation of the infection that occurs in humans, and by understanding which genes do not correlate between humans and mice, we can further understand the limitations of the mouse model.

Mounting evidence suggests that UPEC organisms in the human host rapidly divide (13, 14), and we have recently shown that this high growth rate is recapitulated in the mouse model, although to a lesser degree (13). This difference in growth rate between human and mouse UTIs potentially can be understood by examining the genes that are differentially expressed between human and mouse infections. Most of the differentially expressed genes were expressed at a lower level during hUTI than during mUTI (145 of 175 genes). Many of these 145 genes are involved in anaerobic metabolism. Several of them were clustered in operons encoding oxidoreductases involved in fumarate or nitrite reduction. Additionally, genes involved in nutrient usage under anaerobic conditions were also expressed at a lower level during hUTI, such as the *all* operon, which encodes the catabolic pathway for allantoin degradation (a step in purine catabolism [31]), or the *ula* operon, which encodes both an L-ascorbate transporter and the corresponding enzymes for utilization of L-ascorbate, a compound that can be present in urine due to its water-soluble nature (32). Therefore, we hypothesize that the human bladder is better oxygenated than the mouse bladder. Indeed, a higher oxygen level in human bladders might also account for the higher levels of replication observed in hUTI (13), since an aerobic lifestyle can support more rapid growth. There were also differences in transport systems involved in nutrient acquisition between hUTI and mUTI. Arabinose transport (*araADFGH*) was expressed at a lower level in humans; arabinose has been shown to be present in human bladders in micromolar amounts when normalized to creatine (32). It is also present in murine bladders (33) but has never been precisely quantified. It would be interesting if arabinose is present in smaller amounts in humans than in mice, accounting for this difference in regulation. One of the few genes that was upregulated in humans compared to mice was *dsdX*, which encodes a D-serine transporter. Interestingly, D-serine is present in micromolar amounts in human urine (34), D-serine utilization is associated with uropathogenic strains (35, 36), and accumulation of D-serine leads to a "hypervirulent" phenotype (36, 37) in the urinary tract. Since there was an upregulation in D-serine transport, and not in the deaminase required for its breakdown (*dsdA*), perhaps this presents a mechanism to increase the intracellular levels of D-serine specific to hUTI.

We also compared the gene expression profiles of UPEC during infection with the two most common *in vitro* models, LB cultures and pooled filter-sterilized human urine cultures. Surprisingly, even though urine might seem to be the more physiologically relevant medium for *in vitro* experimentation, LB overall provided a better model for infection than urine cultures. Indeed, the correlations of strains grown in LB approached the correlations found when comparing human infection to the mouse model (Fig. 3). However, there were more differentially regulated genes between hUTI and LB (286 [data not shown]) than between mUTI and hUTI (174 genes). Furthermore, pathway

analysis using the online tool DAVID (38) revealed several pathways that were found to be statistically significantly enriched (enrichment score $\geq$ 1.5) when comparing LB with hUTI (Table S6) or LB with mUTI (Table S6). Several pathways were found to be shared in both comparisons, specifically, iron homeostasis or acquisition as well as motility, and various metabolism pathways (tricarboxylic acid [TCA], arginine and proline, and sulfur) were differentially regulated between the LB and *in vivo* conditions (Table S6). Not only do these results corroborate the results from Fig. 6, but also they point to shared differences between either infection model and the *in vitro* model, further underscoring the similarities between mUTI and hUTI.

A major difference between *in vitro* growth of UPEC in LB or urine is growth rate, and one of the major hallmarks of the transcriptional program of UPEC during infection is rapid growth. When comparing the pathways enriched in the differentially regulated genes between hUTI or mUTI and urine, ribosomes are found to be enriched (Table S7). However, that is just one of seven other statistically significantly pathways that are enriched; there is a variety of factors influencing this outcome. Furthermore, several of these pathways (biosynthesis of amino acids, flavin adenine dinucleotide binding, and nitrogen metabolism/nitrogen utilization) are shared between mUTI versus urine and hUTI versus urine, implying that there are similarities between the two infections that are not observed in *in vitro* growth in urine (Table S7).

There are several factors that vary between infection conditions and *in vitro* growth that could account for the lower correlation between hUTI and urine culture gene expression, for example, a nutrient limitation specific to *in vitro* growth. The bladder is akin to a chemostat, with fresh urine constantly being introduced into the organ, a condition that is not recapitulated under the *in vitro* conditions. Furthermore, the collected urine is typically filter sterilized, and this method excludes exfoliated bladder epithelial cells, likely another major source of nutrients for the pathogen during human infection. In future studies, we could add lysed bladder cells from cell culture to supplement the filter-sterilized urine and determine if this represents a better model of the nutrient milieu. However, when studying specific systems, such as iron acquisition, urine is a better model than LB, since it more accurately recapitulates the iron-limited environment of the host.

In summary, while both *in vitro* models have advantages and disadvantages, the mouse model offers a holistic representation of infection and accurately models UPEC pathway expression. Detailed examination of gene expression profiles between mice and humans allows us to understand which parts of the model are not recapitulated in patients, so we may tailor our studies accordingly. This way the mouse model can serve as a platform to answer questions that are more difficult or impossible to assess when working with human patients.

MATERIALS AND METHODS

Bacterial culture conditions. Clinical UPEC strains HM43, HM56, and HM86 (30) were cultured overnight in LB medium at 37°C with aeration. The next morning, cultures were centrifuged and the pellets washed twice with PBS and then diluted 1:100 into either fresh LB medium or human urine. The human urine was collected and pooled from at least four healthy female volunteers and passed through a 0.22-μm filter for sterilization. Bacteria were cultured at 37°C with aeration to mid-exponential phase (~3 h) and then stabilized in RNAprotect (Qiagen). Bacterial pellets were stored at −80°C until RNA isolation.

Mouse infection. Forty female CBA/J mice were transurethrally inoculated, using the previously established ascending model of UTI (8), with 10^8 CFU of either HM43, HM56, or HM86 that had been cultured in LB overnight with shaking. The infection was allowed to progress for 48 h. Urine from five mice was collected to enumerate bacterial burden, while the rest was collected for RNA (see below for method). Mice were sacrificed, and their bladders and kidneys were aseptically removed, homogenized, and plated to determine bacterial burden. Mouse urine was collected as previously described (13). Briefly, at 48 hpi, urine was directly collected into RNAprotect, pooled, and pelleted. This was repeated every 45 min five more times, resulting in a total of six pellets. These pellets were stored at −80°C until RNA isolation.

RNA isolation and library preparation. RNA was isolated as previously described (13). Briefly, all bacterial pellets were treated with both lysozyme and proteinase K, and then total RNA was extracted using an RNeasy kit (Qiagen). Genomic DNA was removed using the Turbo DNA-free kit (Thermo Fisher). Eukaryotic mRNA was depleted using Dynabeads covalently linked with oligo(dT) (Thermo Fisher). The

TABLE 3 Scoring criteria for histopathological analysis

	Description for score			
Lesion	**0**	**1**	**2**	**3**
Cystitis	No scorable lesions	Very rare PMNs[a] in stroma or lumen or occasional perivascular lymphoid cuffs	Many PMNs and moderate edema	Many PMNs; widespread, marked edema, transmural inflammation
Pyelonephritis	No scorable lesions	Very occasional PMNs in lumen or peripelvic tissue	Rafts of PMNs in the pelvis and/or scattered focal aggregates of PMNs in peripelvic tissue	Many PMNs in all sections, or a single large focus of PMNs in one section

[a]PMNs, polymorphonuclear leukocytes.

in vitro samples underwent the same treatment with Dynabeads to reduce any potential biases this procedure might have introduced to the downstream sequencing. The supernatant was collected from this treatment, and RNA was concentrated and repurified using the RNA Clean and Concentrator kit (Zymo).

To compare the results of the new RNA-sequencing experiment to the published expression data obtained with the human samples (13), the library preparation method needs to be identical to avoid batch effects. The original sequencing data (hUTI) were obtained using the ScriptSeq Complete kit (bacteria) to prepare the cDNA library. However, at the time of this study, Illumina had discontinued this kit. Therefore, we needed to use any leftover kits that had the same base preparation method (ScriptSeq). To accomplish this, we used the ScriptSeq Complete Gold kit (epidemiology), which also contains rRNA removal for bacteria and eukaryotes for the HM86 mouse sample and all three HM43 samples (mouse, LB, and urine). ScriptSeq Complete (bacteria) was used on the HM56 mouse sample, where the kit contained rRNA removal for bacteria; mammalian rRNA was removed with Thermo Fisher's mammalian rRNA removal kit (catalog number 457012). Then the *in vitro* samples from both HM56 and HM86 were prepared using the ScriptSeq Complete (bacteria) kit, which removes bacterial rRNA.

RNA sequencing. *E. coli* HM43 was sequenced using Illumina HiSeq2500 (single end; 50-bp read length), and *E. coli* HM56 and HM86 were sequenced using Nextseq-500 under identical conditions (single end; 50-bp read length).

Histology and tissue processing. Bladders were removed and halved by cutting on the transverse plane, while kidneys were cut on the sagittal plane. One half of each organ was used to enumerate CFU, while the other half was placed into tissue cassettes and immersion fixed in 10% formalin for at least 24 h. The halves were then embedded in paraffin, cut into thin sections, and stained with hematoxylin and eosin (H&E) by the *In Vivo* Animal Core at the University of Michigan. Tissue sections were scored as described in Table 3. Briefly, this is a scale of 0 to 3, where 0 is no inflammation and 3 is severe inflammation. Each organ section was scored by two different people in a blinded manner, and the scores were averaged.

RNA-seq data processing. A custom bioinformatics pipeline was used for the analysis (https://github.com/ASintsova/rnaseq_analysis). Raw fastq files were processed with Trimmomatic (21) to remove adapter sequences and analyzed with FastQC to assess sequencing quality. Mapping was done with bowtie2 aligner (39) using default parameters. Alignment details can be found in Table S1. Read counts were calculated using HTseq htseq-count (40).

Pearson correlation coefficient calculation, PCA, and hierarchical clustering analysis. For PCA and correlation analysis, transcripts per million (TPMs) were calculated for each gene; TPM distribution was then normalized using $\log_2$ transformation, and these normalized data were used for both PCA and correlation and hierarchical clustering analysis. Pearson correlation and PCA were performed using the Python sklearn library. Hierarchical clustering was performed using Ward's method and Euclidean distance. All of the analyses were also performed using centered log-ratio transformation (instead of $\log_2$ transformation), which has recently been proposed for compositional data, and yielded similar results (these results can be found in Jupyter notebook associated with this article). Jupyter notebooks used to generate the figures are available at https://github.com/ASintsova/upec_mouse_model.

Differential expression analysis. Differential expression analysis was performed using the DESeq2 R package (19). Genes with a $\log_2$ fold change of greater than 1 or less than -1 and adjusted *P* values (Benjamini-Hochberg adjustment) of less than 0.05 were considered to be differentially expressed. Pathway analysis was performed using R package topGO (41).

Data availability. Jupyter notebooks as well as all the data used to generate the figures in this paper are available on github: https://github.com/ASintsova/upec_mouse_model.

SUPPLEMENTAL MATERIAL

Supplemental material is available online only.

FIG S1, TIF file, 2.5 MB.

FIG S2, TIF file, 0.5 MB.

FIG S3, TIF file, 1 MB.

TABLE S1, XLSX file, 0.01 MB.

TABLE S2, XLSX file, 0.02 MB.

TABLE S3, XLSX file, 0.02 MB.
TABLE S4, XLSX file, 0.02 MB.
TABLE S5, XLSX file, 0.02 MB.
TABLE S6, XLSX file, 0.01 MB.
TABLE S7, XLSX file, 0.01 MB.

REFERENCES

1. Flores-Mireles AL, Walker JN, Caparon M, Hultgren SJ. 2015. Urinary tract infections: epidemiology, mechanisms of infection and treatment options. Nat Rev Microbiol 13:269–284. https://doi.org/10.1038/nrmicro3432.
2. Foxman B. 1990. Recurring urinary tract infection: incidence and risk factors. Am J Public Health 80:331–333. https://doi.org/10.2105/ajph.80.3.331.
3. Foxman B. 2010. The epidemiology of urinary tract infection. Nat Rev Urol 7:653–660. https://doi.org/10.1038/nrurol.2010.190.
4. Terlizzi ME, Gribaudo G, Maffei ME. 2017. Uropathogenic *Escherichia coli* (UPEC) infections: virulence factors, bladder responses, antibiotic, and non-antibiotic antimicrobial strategies. Front Microbiol 8:1566. https://doi.org/10.3389/fmicb.2017.01566.
5. Subashchandrabose S, Mobley HLT. 2015. Virulence and fitness determinants of uropathogenic *Escherichia coli*. Microbiol Spectr 3:UTI-0015-2012. https://doi.org/10.1128/microbiolspec.UTI-0015-2012.
6. Sivick KE, Mobley HLT. 2010. Waging war against uropathogenic *Escherichia coli*: winning back the urinary tract. Infect Immun 78:568–585. https://doi.org/10.1128/IAI.01000-09.
7. Alteri CJ, Mobley HLT. 2015. Metabolism and fitness of urinary tract pathogens. Microbiol Spectr 3:MBP-0016-2015. https://doi.org/10.1128/microbiolspec.MBP-0016-2015.
8. Hagberg L, Engberg I, Freter R, Lam J, Olling S, Svanborg Edén C. 1983. Ascending, unobstructed urinary tract infection in mice caused by pyelonephritogenic *Escherichia coli* of human origin. Infect Immun 40:273–283. https://doi.org/10.1128/IAI.40.1.273-283.1983.
9. Seok J, Warren HS, Cuenca AG, Mindrinos MN, Baker HV, Xu W, Richards DR, McDonald-Smith GP, Gao H, Hennessy L, Finnerty CC, López CM, Honari S, Moore EE, Minei JP, Cuschieri J, Bankey PE, Johnson JL, Sperry J, Nathens AB, Billiar TR, West MA, Jeschke MG, Klein MB, Gamelli RL, Gibran NS, Brownstein BH, Miller-Graziano C, Calvano SE, Mason PH, Cobb JP, Rahme LG, Lowry SF, Maier RV, Moldawer LL, Herndon DN, Davis RW, Xiao W, Tompkins RG, Inflammation, and Host Response to Injury, Large Scale Collaborative Research Program. 2013. Genomic responses in mouse models poorly mimic human inflammatory diseases. Proc Natl Acad Sci U S A 110:3507–3512. https://doi.org/10.1073/pnas.1222878110.
10. O'Brien VP, Hannan TJ, Nielsen HV, Hultgren SJ. 2016. Drug and vaccine development for the treatment and prevention of urinary tract infections. Microbiol Spectr 4:UTI-0013-2012. https://doi.org/10.1128/microbiolspec.UTI-0013-2012.
11. Snyder JA, Haugen BJ, Buckles EL, Lockatell CV, Johnson DE, Donnenberg MS, Welch RA, Mobley HLT. 2004. Transcriptome of uropathogenic *Escherichia coli* during urinary tract infection. Infect Immun 72:6373–6381. https://doi.org/10.1128/IAI.72.11.6373-6381.2004.
12. Hagan EC, Lloyd AL, Rasko DA, Faerber GJ, Mobley HLT. 2010. *Escherichia coli* global gene expression in urine from women with urinary tract infection. PLoS Pathog 6:e1001187. https://doi.org/10.1371/journal.ppat.1001187.
13. Sintsova A, Frick-Cheng AE, Smith S, Pirani A, Subashchandrabose S, Snitkin ES, Mobley H. 2019. Genetically diverse uropathogenic *Escherichia coli* adopt a common transcriptional program in patients with UTIs. Elife 8:e49748. https://doi.org/10.7554/eLife.49748.
14. Forsyth VS, Armbruster CE, Smith SN, Pirani A, Springman AC, Walters MS, Nielubowicz GR, Himpsl SD, Snitkin ES, Mobley HLT. 2018. Rapid growth of uropathogenic *Escherichia coli* during human urinary tract infection. mBio 9:e00186-18. https://doi.org/10.1128/mBio.00186-18.
15. Bielecki P, Muthukumarasamy U, Eckweiler D, Bielecka A, Pohl S, Schanz A, Niemeyer U, Oumeraci T, von Neuhoff N, Ghigo J-M, Häussler S. 2014. *In vivo* mRNA profiling of uropathogenic *Escherichia coli* from diverse phylogroups reveals common and group-specific gene expression profiles. mBio 5:e01075-14. https://doi.org/10.1128/mBio.01075-14.
16. Dennis PP, Ehrenberg M, Bremer H. 2004. Control of rRNA synthesis in *Escherichia coli*: a systems biology approach. Microbiol Mol Biol Rev 68:639–668. https://doi.org/10.1128/MMBR.68.4.639-668.2004.
17. Klumpp S, Scott M, Pedersen S, Hwa T. 2013. Molecular crowding limits translation and cell growth. Proc Natl Acad Sci U S A 110:16754–16759. https://doi.org/10.1073/pnas.1310377110.
18. Burnham P, Dadhania D, Heyang M, Chen F, Westblade LF, Suthanthiran M, Lee JR, De Vlaminck I. 2018. Urinary cell-free DNA is a versatile analyte for monitoring infections of the urinary tract. Nat Commun 9:2412. https://doi.org/10.1038/s41467-018-04745-0.
19. Love MI, Huber W, Anders S. 2014. Moderated estimation of fold change and dispersion for RNA-seq data with DESeq2. Genome Biol 15:550. https://doi.org/10.1186/s13059-014-0550-8.
20. Jones PG, VanBogelen RA, Neidhardt FC. 1987. Induction of proteins in response to low temperature in *Escherichia coli*. J Bacteriol 169:2092–2095. https://doi.org/10.1128/jb.169.5.2092-2095.1987.
21. Goldstein J, Pollitt NS, Inouye M. 1990. Major cold shock protein of *Escherichia coli*. Proc Natl Acad Sci U S A 87:283–287. https://doi.org/10.1073/pnas.87.1.283.
22. Brandi A, Pon CL. 2012. Expression of *Escherichia coli cspA* during early exponential growth at 37°C. Gene 492:382–388. https://doi.org/10.1016/j.gene.2011.10.047.
23. Yamanaka K, Inouye M. 2001. Induction of CspA, an *E. coli* major cold-shock protein, upon nutritional upshift at 37 degrees C. Genes Cells 6:279–290. https://doi.org/10.1046/j.1365-2443.2001.00424.x.
24. Pos KM, Dimroth P, Bott M. 1998. The *Escherichia coli* citrate carrier CitT: a member of a novel eubacterial transporter family related to the 2-oxoglutarate/malate translocator from spinach chloroplasts. J Bacteriol 180:4160–4165. https://doi.org/10.1128/JB.180.16.4160-4165.1998.
25. Lane MC, Alteri CJ, Smith SN, Mobley HLT. 2007. Expression of flagella is coincident with uropathogenic *Escherichia coli* ascension to the upper urinary tract. Proc Natl Acad Sci U S A 104:16669–16674. https://doi.org/10.1073/pnas.0607898104.
26. Alteri CJ, Smith SN, Mobley HLT. 2009. Fitness of Escherichia coli during urinary tract infection requires gluconeogenesis and the TCA cycle. PLoS Pathog 5:e1000448. https://doi.org/10.1371/journal.ppat.1000448.
27. Hagberg L, Hull R, Hull S, Falkow S, Freter R, Svanborg Edén C. 1983. Contribution of adhesion to bacterial persistence in the mouse urinary tract. Infect Immun 40:265–272. https://doi.org/10.1128/IAI.40.1.265-272.1983.
28. Kunin CM, Polyak F, Postel E. 1980. Periurethral bacterial flora in women. Prolonged intermittent colonization with Escherichia coli. JAMA 243:134–139. https://doi.org/10.1001/jama.1980.03300280032024.
29. Zhang D, Zhang G, Hayden MS, Greenblatt MB, Bussey C, Flavell RA, Ghosh S. 2004. A Toll-like receptor that prevents infection by uropathogenic bacteria. Science 303:1522–1526. https://doi.org/10.1126/science.1094351.
30. Subashchandrabose S, Hazen TH, Brumbaugh AR, Himpsl SD, Smith SN, Ernst RD, Rasko DA, Mobley HLT. 2014. Host-specific induction of *Escherichia coli* fitness genes during human urinary tract infection. Proc Natl Acad Sci U S A 111:18327–18332. https://doi.org/10.1073/pnas.1415959112.
31. Xi H, Schneider BL, Reitzer L. 2000. Purine catabolism in *Escherichia coli* and function of xanthine dehydrogenase in purine salvage. J Bacteriol 182:5332–5341. https://doi.org/10.1128/jb.182.19.5332-5341.2000.
32. Bouatra S, Aziat F, Mandal R, Guo AC, Wilson MR, Knox C, Bjorndahl TC, Krishnamurthy R, Saleem F, Liu P, Dame ZT, Poelzer J, Huynh J, Yallou FS, Psychogios N, Dong E, Bogumil R, Roehring C, Wishart DS. 2013. The human urine metabolome. PLoS One 8:e73076. https://doi.org/10.1371/journal.pone.0073076.
33. Justice SS, Lauer SR, Hultgren SJ, Hunstad DA. 2006. Maturation of intracellular *Escherichia coli* communities requires SurA. Infect Immun 74:4793–4800. https://doi.org/10.1128/IAI.00355-06.

34. Brückner H, Haasmann S, Friedrich A. 1994. Quantification of D-amino acids in human urine using GC-MS and HPLC. Amino Acids 6:205–211. https://doi.org/10.1007/BF00805848.
35. Korte-Berwanger M, Sakinc T, Kline K, Nielsen HV, Hultgren S, Gatermann SG. 2013. Significance of the D-serine-deaminase and D-serine metabolism of *Staphylococcus saprophyticus* for virulence. Infect Immun 81:4525–4533. https://doi.org/10.1128/IAI.00599-13.
36. Roesch PL, Redford P, Batchelet S, et al. 2003. Uropathogenic *Escherichia coli* used-serine deaminase to modulate infection of the murine urinary tract. Mol Microbiol 49:55–67. https://doi.org/10.1046/j.1365-2958.2003.03543.x.
37. Anfora AT, Haugen BJ, Roesch P, Redford P, Welch RA. 2007. Roles of serine accumulation and catabolism in the colonization of the murine urinary tract by *Escherichia coli* CFT073. Infect Immun 75:5298–5304. https://doi.org/10.1128/IAI.00652-07.
38. Huang da W, Sherman BT, Lempicki RA. 2009. Systematic and integrative analysis of large gene lists using DAVID bioinformatics resources. Nat Protoc 4:44–57. https://doi.org/10.1038/nprot.2008.211.
39. Langmead B, Salzberg SL. 2012. Fast gapped-read alignment with Bowtie 2. Nat Methods 9:357–359. https://doi.org/10.1038/nmeth.1923.
40. Anders S, Pyl PT, Huber W. 2015. HTSeq—a Python framework to work with high-throughput sequencing data. Bioinformatics 31:166–169. https://doi.org/10.1093/bioinformatics/btu638.
41. Alexa A, Rahnenfuhrer J. 2018. topGO: enrichment analysis for gene ontology. R package version 2.34.0.